Chemical Physics 92 (1985) 457–470
North-Holland, Amsterdam

PHOTOIONIZATION STUDY OF THE CN ANION: A STUDY OF THE NaCN(001) SURFACE IN COMPARISON WITH CO AND N_2 [1]

H. PULM [2], B. MARQUARDT [2], H.-J. FREUND [3]

Institut für Physikalische und Theoretische Chemie, Universität Erlangen-Nürnberg, Egerlandstrasse 3, D-8520 Erlangen, FRG

R. ENGELHARDT

II. Institut für Experimentalphysik, Universität Hamburg, Luruper Chaussee 149, D-2000 Hamburg 50, FRG

K. SEKI [4], U. KARLSSON [5], E.E. KOCH

Hamburger Synchrotronstrahlungslabor HASYLAB at DESY, Notkestrasse 85, D-2000 Hamburg 52, FRG

and

W. VON NIESSEN

Institut für Physikalische und Theoretische Chemie, Technische Universität Braunschweig, Hans-Sommer Strasse 10, D-3300 Braunschweig, FRG

Received 25 June 1984

The results of a combined synchrotron UV-radiation and conventional XPS study on the (001) surface of a NaCN single crystal are reported. Absolute valence and core binding energies of CN^- are deduced. The valence electron spectrum of NaCN is shown to be dominated by emission from the CN^- sublattice. Satellite structure is found in the inner valence electron region and consistently interpreted in comparison with CO and N_2. The experimentally determined electronic structure is compared with many-body ab initio calculations of the ionization spectrum of CN^-. No band structure effects (k dispersion) in the valence spectra are found due to the rotational disorder of the CN sublattice. The branching ratios of the outer valence levels are determined, and shape resonances in both σ levels are observed. The energies of the shape resonances in CN^- are compared with gaseous, condensed and adsorbed CO and N_2.

1. Introduction

In recent years much progress has been made in the understanding of the photoionization process in diatomic molecules, such as CO and N_2, in the gas phase [1], the condensed solid phase [2] and in adsorbate phases [1].

Of particular interest has been the energy dependence of the photoionization cross section since the observation of molecular shape resonances [3]. It has been shown recently, that energetic position and intensity of such shape resonances are considerably influenced by binding the free molecule to a metal surface [1,4]. Firstly, this could be due to the change of the potential felt by the escaping electron caused by a redistribution of the electron density upon binding a molecule to the surface, i.e.

[1] Work supported in part by Bundesministerium für Forschung und Technologie (BMFT) from funds for research with synchrotron radiation.

[2] Present address: Lehrstuhl für Theoretische Chemie, Universität zu Köln, Greinstrasse 4, D-5000 Cologne 41, FRG.

[3] To whom correspondence should be addressed.

[4] Permanent address: Institute for Molecular Science, Myodaiji, Okazaki 444, Japan.

[5] Permanent address: Department of Physics, Linköping University, S-58183 Linköping, Sweden.

initial state effects. Secondly, possibly even more important, relaxation of the final ion state may determine the observed energetic position of such resonances. Also, scattering from the surface will have an effect on intensity and energy of shape resonances.

Another point of current interest, that has attracted the attention of both theoreticians [5] and experimentalists [6,7], is the explanation of satellite structure found in the inner valence electron region. Very recently, the energy dependence of the intensity of these satellites in N_2 and CO have been studied in the gas and condensed phases [6,7].

In this study we want to investigate the photoionization of CN^-. We have chosen this system for two reasons:

(i) CN^- is isoelectronic with CO and N_2.

(ii) The electron distribution in CN^- is different from CO and N_2 [8–12].

The photoionization of CN^- therefore allows us to investigate the influence of the altered charge distribution on position and intensity of the photoemission bands including the satellite structure in the inner valence region. Furthermore it serves as a model to study the influence of the altered wavefunction on the position of the shape resonance. By means of a comparison of the results for CN with CO^- and N_2 we might have the chance to differentiate between initial and final state effects on energetic position and intensity of molecular shape resonances.

Since CN^- is an anion its study in the gas phase is hampered. CN^-, however, forms stable alkalicyanide crystals with rock-salt structure at room temperature as shown in fig. 1a [13,14]. Due to the large electron affinity (3.82 eV [15]) of CN^-, which is even larger than that of fluorine, the rock-salt lattice points of NaCN, for example, are occupied by Na cations and the bary centers of the CN^- anions, respectively. An oriented CN moiety would not allow for the high cubic symmetry of a rock-salt crystal. The cubic symmetry originates from the rotational mobility of the CN units [14,16]. The rotational distribution, however, is not isotropic as shown in fig. 1b, which has been taken from the neutron-diffraction study of Rowe et al. [16]. To a certain degree we can therefore

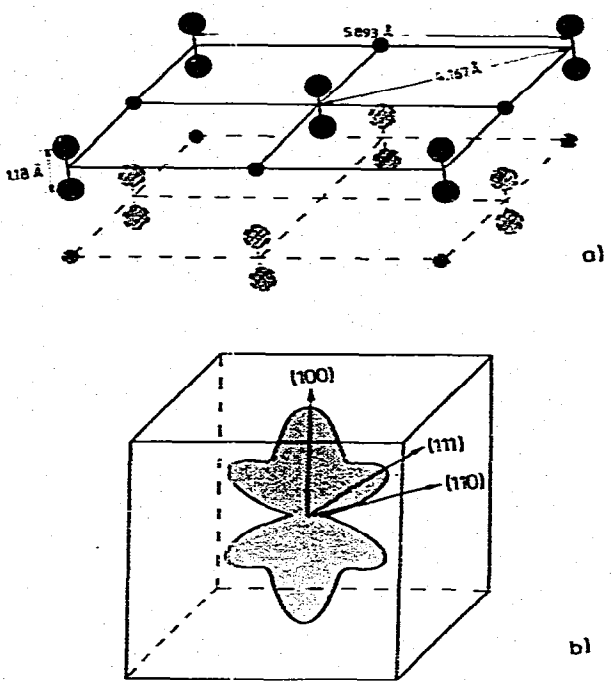

Fig. 1. (a) Schematic representation of the crystal structure of the cubic phase of NaCN. Only the first two layers of a (100) surface are shown [13]. (b) Angular dependence of the density of C and N atoms on a sphere of radius one half of the CN bond length. The cube indicates the various directions within the crystal [16].

consider a NaCN crystal at room temperature as a condensed Coulomb stabilized CN^- gas, where the intermolecular separation between the CN^- moieties is ≈ 4.2 Å.

On pressure and temperature variation NaCN and other alkalicyanides undergo several phase transitions. At a transition temperature of 288 K the rotational freedom of the CN^- anions is frozen along the [110] direction [17] and the mechanical properties change rather dramatically. Recently, there is a wide interest in alkalicyanides from this point of view [18].

Using angle-resolved photoemission with synchrotron radiation and angle-integrated X-ray photoelectron spectroscopy we investigate the complete outer and inner valence electron region as well as the CN^- core ionizations of a (100)

surface of a NaCN single crystal in normal emission. By comparison with solid and gaseous CO and N_2 relative binding energy differences and branching ratios intermediate between CO and N_2 are found. We observe satellite structure in the inner valence electron region and present an assignment analogous to CO and N_2 [7] in comparison with many-body ab initio calculations. It is found that the relative ionization potential of the CN σ bond is lowered with respect to the lone pairs in comparison with CO and N_2 by ≈ 3 eV which is in line with theoretical predictions based on one-particle properties.

The determined branching ratios of the three ion states lowest in energy in normal emission are compared with CO and N_2 and angle-integrated measurements using unpolarized resonance lamp radiation [19]. The comparison indicates that we observe the influence of the anisotropic orientation of the CN^- moieties. The branching ratios determined in normal emission show shape-resonance structures that are shifted in energy relative to those of CO and N_2.

The paper is organized as follows: In section 2 we review the experimental procedures. Section 3 briefly summarizes the calculational details. In section 4 we discuss the experimental results and compare them with results in the literature and our own theoretical considerations. Also, a brief excursion to adsorbates is presented. Section 5 contains a synopsis.

2. Experimental procedure

The synchrotron experiments were performed at the storage ring DORIS in Hamburg. The synchrotron light was dispersed by a 1m Seya–Namioka monochromator with concave gratings. The photon flux was monitored with a photodiode during the measurements. We recorded the electron distribution curves with a modified VG(ADES 400)-system in normal emission with an angular resolution of $\pm 1°$. The overall resolution was $\Delta E = 0.25$ eV for $h\nu < 40$ eV, $\Delta E = 0.4$ eV for $h\nu = 40$ eV and $\Delta E = 0.55$ eV for $h\nu = 45$ eV. A detailed description of the experimental arrangement can be found in ref. [20]. Photoemission experiments using a conventional X-ray with Mg- and Si-anodes were performed in a separate system using a modified Leybold–Heraeus (LHS 10) spectrometer [21]. The sample was a highly purified NaCN single crystal which was cleaved "in vacuo" along the [100] direction within a preparation chamber. After cleavage the sample was transferred under UHV into the measuring position. In order to fix the

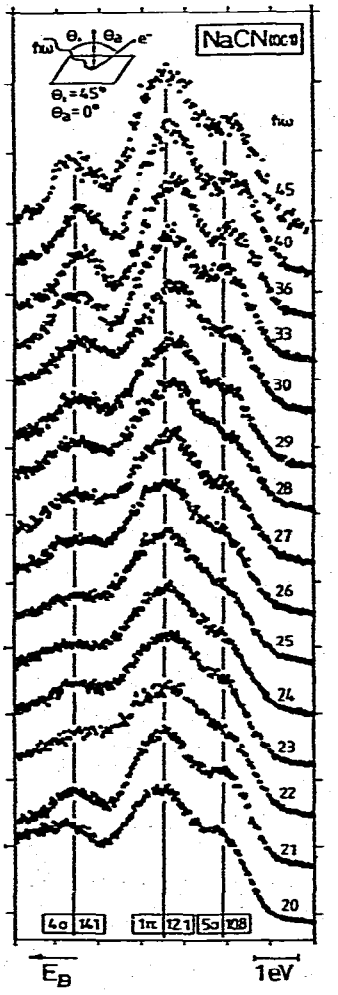

Fig. 2. Set of angle-resolved photoelectron spectra taken with synchrotron radiation for different excitation energies. The geometry of the experiment is indicated. The absolute binding energies of the three outer valence electron levels are given at the bottom (in eV).

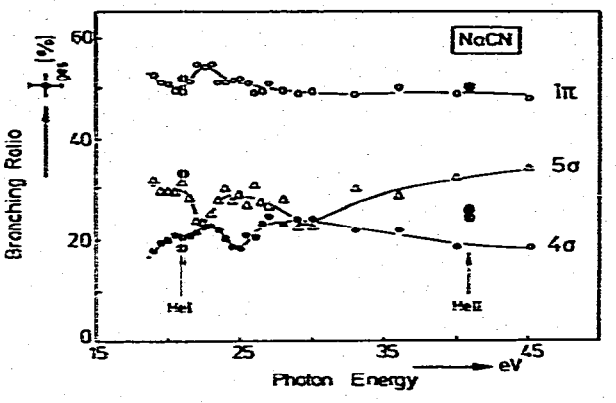

Fig. 3. Branching ratios for the three outer valence levels between 20 and 45 eV photon energy.

crystal onto the sample holder it was pressed into metallic indium. The pressure in the system was kept in the 10^{-10} Torr range.

Typical photoelectron distribution curves from the NaCN crystal are shown in fig. 2. They have been measured at room temperature. The zero of the intensity scale refers to the spectrum at the bottom. The energy scale was fixed with respect to the values reported for metallic indium [22] *.

For evaluating the branching ratios $B^i = A_i / \Sigma_i A_i$ where A_i is the emission intensity of the ith state and the sum is over all observed states of the ion the data were further processed. For the determination of photoemission intensities the electron distribution curves for each excitation energy were normalized to the intensity of the photon flux impinging onto the sample. Furthermore a smooth structureless background was subtracted to account for scattered secondary electrons. Finally, the area under each emission peak in the electron distribution curves was determined by fitting the experimentally observed three-peak structure by three gaussians corresponding to the three uppermost ion states. The branching ratios are plotted in fig. 3 as a function of photon energy.

* Values used are 17.64 eV/16.74 eV.

3. Computational procedures

Standard LCAO MO SCF calculations were carried out for CO, N_2 and CN^- using the ORBIT-84 program [23], specifically designed for ab initio calculations on a simple micro computer. All integrals were calculated analytically over cartesian gaussian-type functions [24,25]. Two basis sets, i.e. a minimal basis, STO-3G [26], and a split-valence basis, 3-21G [27], were employed. No further optimization was tried for the 3-21G basis set. For the STO-3G basis set the π-orbital exponents were slightly altered, due to their strong influence on orbital and total energies. There are reports of better calculations [10], but they are not directly comparable for the three systems. All calculations were carried out using experimental geometries. The results for the three systems with the 3-21G basis are collected in table 1.

In addition to these calculations Green's function computations have been performed on the CN anion at an intermolecular separation of 0.118 nm. The Green's function calculations are based on ab initio SCF calculations and include the effects of electronic correlation and reorganization. Two types of approximations in the framework of the Green's function method have been employed. The first method is based on a finite perturbation expansion of the self-energy. All terms up to and including the third-order terms in the electron–electron interaction are taken into account. Higher-order terms are approximated by a renormalization procedure. The method, however, is only applicable in the outer valence region, and is thus termed outer valence Green's function method (OVGF). It is discussed in detail in refs. [28,29]. The accuracy achievable is documented in ref. [30]. If satellites of appreciable intensity accompany the main lines the ionization energies and relative intensities have to be calculated with the so-called extended two-particle–hole Tamm–Dancoff Green's function method (extended 2ph–TDA). This method can be used in the entire valence region. It is also accurate to third order in the electron–electron interaction and contains infinite selected summations such that the self-energy retains the correct analytical structure over the entire energy range. The method is extensively

Table 1
Hartree–Fock orbital energies for CO, N_2 and CN^- (in eV) using a 3-21G basis set. Column I contains the absolute, column II the relative orbital energies (see text). For each molecule the total energy is given at the bottom. The valence-electron orbital energies of CN^- calculated with a [12s/8p/2d] basis are shown in addition

Sym	CO		N_2		CN^-		
	I E_{orb}(eV)	II E_{rel}(eV)	I E_{orb}(eV)	II E_{rel}(eV)	I E_{orb}(eV)	II E_{rel}(eV)	E_{orb}(eV) [12s/8p/2d]
1σ	−559.747	538.385	−424.601	403.872	−411.774	404.260	–
2σ	−307.841	286.479	−424.576	403.847	−294.689	287.175	–
3σ	−42.841	20.734	−41.317	20.729	−24.381	16.867	−25.322
4σ	−21.362	0.0	−20.588	0.0	−7.514	0.0	−9.249
1π	−17.266	−4.095	−16.853	−3.735	−2.933	−3.583	−5.302
5σ	−14.777	−6.585	−16.762	−3.826	−3.531	−3.983	−5.251
2π	4.397	–	5.058	–	15.096	–	–
6σ	13.388	–	20.720	–	23.051	–	–
E_{tot}	−134.591064 au		−132.243149 au		−110.909348 au		–

discussed [31] (for an earlier version of this method see refs. [29,32]). The numerical aspects have been presented in ref. [33]. The Green's function calculations are based on an SCF calculation which uses a large basis set including diffuse functions and two sets of d-type polarization functions, namely [12s8p2d]/(6s5p2d) which is derived from a basis set by Salez and Veillard [34]. The SCF calculations were performed with the program MUNICH of Diercksen and Kraemer [35]. The orbital energies are shown in table 1. The results of the OVGF and the extended 2ph–TDA calculations are presented in table 2. The basis set has been fully exhausted in the OVGF calculation but had to be slightly truncated in the extended 2ph–TDA calculation. The two core orbitals (C1s and N1s) and their virtual counterparts have been neglected. In addition, virtual orbitals with an

Table 2
Results of the extended 2ph–TDA calculation on CN^- using the [12s/8p/2d] basis set. The ionization potentials (IP) given in parentheses are calculated using the OVGF method [29]. Pole strengths (ps) are given for the extended 2ph–TDA results. The hole states given in parentheses are those to which the given excited configurations couple

Sym	IP	PS	Hole	2ph excitation [a]
states of σ symmetry	4.11 (3.81)	0.87	5σ	
	7.55	0.81	4σ	
	13.01	0.053	(4σ)	$5\sigma^{-1}1\pi^{-1}\pi^*$
	17.80	0.068	(3σ)	$5\sigma^{-1}1\pi^{-1}\pi^*, 5\sigma^{-2}\sigma^*$
	18.46	0.059	(3σ)	$4\sigma^{-1}1\pi^{-1}\pi^*$, ...
	18.88	0.009	(3σ)	
	22.72	0.074	(3σ)	$5\sigma^{-1}1\pi^{-1}\pi^*, 4\sigma^{-1}1\pi^{-1}\pi^*$
	23.31	0.150	(3σ)	$4\sigma^{-1}5\sigma^{-1}\sigma^*, 5\sigma^{-2}\sigma^*$
				$4\sigma^{-2}\sigma^*, 1\pi^{-2}\pi^*$
states of π symmetry	5.60 (5.11)	0.88	1π	
	17.68	0.008	(1π)	$1\pi^{-1}5\sigma^{-1}\sigma^*$

[a] σ^*, π^* denote virtual orbitals of these symmetries. Because the basis set contains Rydberg functions they are in general not the lowest virtual orbitals of this symmetry. It is, however, obvious from the calculation that excitations into Rydberg-type orbitals also do contribute although they are not dominant.

energy above 46 eV were left out in the latter calculation.

4. Results and discussion

4.1. Energetic considerations and satellite structure

We start the discussion with a comparison of the outer and inner valence emission of NaCN at 45 and 1253.6 eV photon energy with the spectra of condensed CO and N_2 [7] shown in fig. 4. Note, however, that while the NaCN 45 eV spectrum was taken in an angle-resolved mode in normal emission, the spectra of condensed CO and N_2 and the 1253.6 eV spectrum of NaCN are angle-integrated [7].

For the comparison we have chosen a relative energy scale, where the maximum of the 4σ state * has been taken as reference level. This is indicated by the dash-dotted line in fig. 4. Table 3 contains the relative binding energies of NaCN, CO and N_2.

One result is obvious: the complete valence emission of the NaCN single crystal is determined by ion states due to ionization of the CN^- anion, as expected. The Na2p emission is observed well below (= 23 eV) the valence band. This result supports the view that a complete charge transfer between Na and CN moiety has taken place. Our spectra are in fair agreement with the spectra reported by Considine et al. [19] and Vannerberg [36] who measured HeI and HeII [19] spectra as well as monochromatized AlKα [36] spectra respectively of polycrystalline films of sodium cyanide. The relative binding energies of the three outer valence ionizations are intermediate between CO and N_2; however, they are more similar to N_2 than to CO. In addition the relative intensities of the three peaks of CN^- are more similar to N_2 than to CO which is evident by inspection of fig. 4. If we excite the valence electrons with soft X rays, the molecular states with large atomic s character [37] are intensity enhanced, while those with dominating atomic p character appear to be inten-

* The CO one-particle nomenclature is used throughout the paper for CO, N_2 and CN^-.

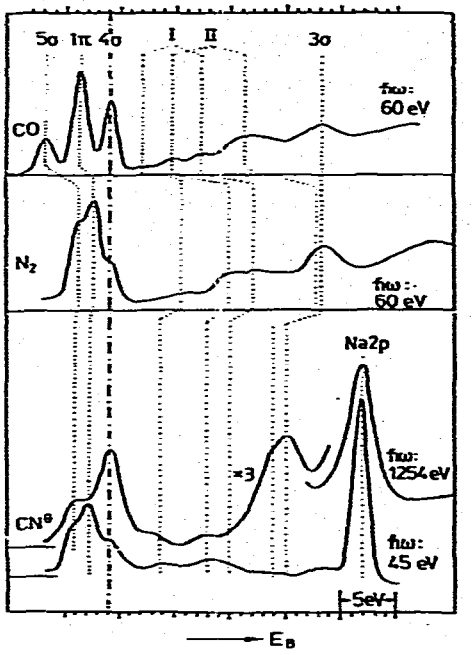

Fig. 4. Comparison of the valence photoelectron spectra of NaCN taken with 45 eV (normal emission) and 1253.6 eV(angle-integrated) photon energies with those of condensed CO and N_2 [7]. The spectra have been alligned at the maximum of the 4σ emission.

Table 3
Experimental ionization energies for CO, N_2 and NaCN relative to the position of the 4σ state. Negative values refer to lower, positive values to higher relative binding energies

State	CO	NaCN	N_2
5σ	−5.98	−3.33	−2.93
1π	−2.79	−2.0	−1.46
4σ	0.0	0.0	0.0
	2.93	4.66	6.52
	5.59	8.91	10.77
	8.25	10.91	13.03
	12.24	14.90	18.75
3σ	19.29	16.23	19.42
Na2p		23.14	
C1s	275.8 [a]	276.10	
N1s		391.64	391.3 [a]
O1s	522.0 [a]		

[a] Ref. [38].

sity suppressed. The 4σ state with large N2s character dominates the X-ray-excited spectrum, while the 1π emission is drastically reduced. This behaviour is in line with the observations on N_2 and CO [38]. Our assignment of the outer valence levels is at variance with those of several other authors [36,39] who were not able to detect the 1π emission in X-ray-excited spectra. Considine et al. [19], Vannerberg [36] and Prins and Biloen [39] report on electron emission at energies below the three outer valence emissions of NaCN. Vannerberg [36] reports five bands at 2.6, 4.7, 9.4, 16.1 and 23 eV relative binding energy including the Na2p emission. Prins and Biloen [39] found three bands at: 4.7, 14.2 and 22.4 eV below the 4σ emission. Considine et al. [19] were only able to observe one peak ≈ 9 eV below the 4σ band using HeII radiation.

Our results, shown in table 3, are consistent with those of Vannerberg [36]. We do not observe, however, the band at 2.6 eV relative binding energy in our 45 eV spectrum and are not able to resolve a peak in the X-ray-induced spectra. We cannot rule out, experimentally, the possibility of a band at this energy although our calculations, discussed later, do not predict a satellite with this relative binding energy (see fig. 5). The peak at 4.7 eV in the high-energy spectrum is observed as a weak feature with a photon energy of 45 eV. Considine et al. [19] did not observe this band. In several papers, dealing with XPS and NaCN [36,39,40] a peak between 14.5 and 16 eV below the 4σ level has been reported in agreement with our results. This band is due to the emission from the CN σ bond, which in a one-particle picture is termed 3σ. It is interesting that the intensity of this state is close to zero for $h\nu = 45$ eV photon energy in the angle-resolved normal emission spectrum. The strong intensity enhancement of this band supports the high s character of the ionized state in agreement with our assignment to the ionization of the CN σ bond.

At this point it is appropriate to compare the electron emission bands below the outer valence emissions in CN^- with those found in CO and N_2 [7]. In the latter cases assignment has been extensively discussed [5,41,42]. A simplified version [7,43] of the current assignment may be summarized as follows: The coupling of a $\pi \rightarrow \pi^*$ excitation to a hole state of σ symmetry, namely a configuration of type $(\sigma^{-1}\pi^{-1}\pi^*)$ leads to two doublet states whose energy separation is determined by the singlet–triplet splitting of the $\pi \rightarrow \pi^*$ excitation. The lowest-energy $\pi \rightarrow \pi^*$ excitation in the first-row diatomics is the $1\pi \rightarrow 2\pi$ excitation. If we couple this excitation separately to the 5σ and the 4σ hole states we end up with four final states of the type discussed above. The roman numbers I and II (fig. 4) refer to these states where I stands for the 5σ and II for the 4σ coupling. The splitting between the components of each pair is very similar and of the order of 6–8 eV. It is close to the singlet–triplet splitting of the $1\pi \rightarrow 2\pi$ excitation in neutral CO and N_2 [44]. We want to point out clearly, that the above assignment is probably oversimplified. We know from detailed calculations, that a variety of other excited ion configurations, including two-electron

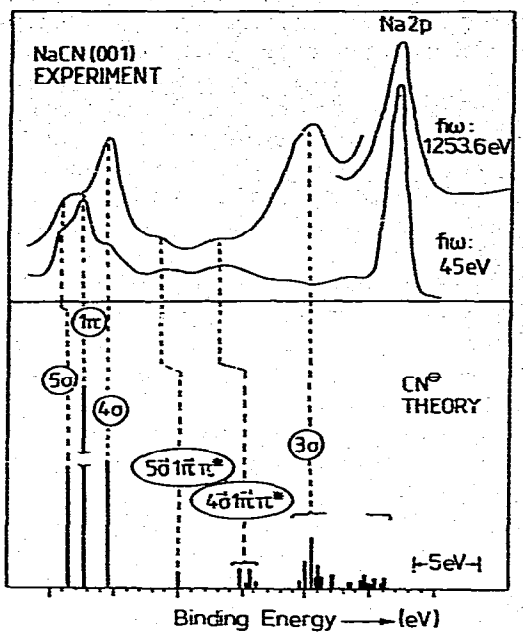

Fig. 5. Comparison of the experimental valence photoelectron spectrum of NaCN with a many-body corrected Hartree–Fock calculation on the CN^- anion. The calculated 4σ ionization energy has been alligned with the experimental 4σ ionization energy.

excitations [46], contribute. This is particularly important for the satellites at higher relative binding energies, close to the 3 ionization. For the satellites at lower binding energies, the above assignment reflects the true situation [41]. The satellites at lower binding energy borrow their intensity from the outer valence levels while those at higher binding energies borrow intensity from the 3σ ionization [7].

A qualitatively similar analysis holds for CO and N_2. The larger excitation energy for the $1\pi \rightarrow 2\pi$ excitation in N_2 as compared to CO has to be taken into account [44]. Note that the splitting of the singlet and triplet component remains basically unaffected. The energy separation between 5σ and 4σ hole states decreases for N_2. As a consequence of these two effects the satellites shift to higher relative binding energies in N_2.

If we now use the assignment for CO and N_2 as a basis to assign the inner valence electron spectrum of NaCN we end up with the dotted correlation lines shown in fig. 4. As a next step to test this assignment we compare our spectrum with the result of an extended 2ph–TDA calculation on the photoelectron spectrum of the outer and inner valence electron region of CN^- (see ref. [45] for comparison). Fig. 5 shows a direct comparison between experiment and theory. Note that the calculation was done on a free CN^- anion. Therefore the energy scales have been alligned for the 4σ bands. The theoretical quantity proportional to the band intensity is the so-called pole strength which is equivalent to a generalized overlap amplitude and thus represents the intensity of an ionization band in sudden approximation [47]. We find two groups of rather intense satellites 5.5 and 10.8 eV below the 4σ ionization and a set of satellites in the region of 3σ ionization. The main configurations contributing to the two satellites at low relative binding energy are of type $(5\sigma^{-1}1\pi^{-1}2\pi)$ for the 5.5 eV band and $(4\sigma^{-1}1\pi^{-1}2\pi)$ for the 10.8 eV band, which is in agreement with the results of our simple considerations. For the satellites in the 3σ ionization region the situation is more complicated, as already found for CO and N_2. The coupling to various configurations leads to the broad, structured peak observed for the 3σ ionization. Still, the 3σ ionization is the most significant contribution to the peak. In comparison to CO and N_2, where the relative position of the 3σ ionization is almost identical, the CN^- 3σ ionization is found at lower binding energy. This can be rationalized on the basis of our ab initio Hartree–Fock calculations (table 1). Columns I of table 1 contain absolute energies, columns II relative energies with respect to the 4σ orbital. The latter energies are in line with the experimental observations on the 3σ ionization from fig. 4 and table 3: the CN^- 3σ orbital is destabilized by ≈ 3 eV with respect to the corresponding orbitals in CO and N_2, which are within 0.1 eV at the same relative energy. The reason for this effect can be found in the electronegativities of the atoms participating in the bond. Roughly, the larger the electronegativity of an atom the larger is the atomic orbital energy [48]. In the three cases, the σ bond is formed by coupling of two atomic sp-hybride functions. In fig. 6 the situation is shown schematically for the three molecules. In CO, the oxygen function lies at high energy due to the large electronegativity of oxygen (3.5) [48]. The occupied σ bond formed by interaction with the less electronegative carbon (2.5) [48] is situated at even higher energy. In N_2 the two interacting hybrides are degenerate and lie at intermediate energy according to the electronegativity of nitrogen (3.0) [48]. Due to the degeneracy of the interacting atomic functions the formed σ bond is more stabilized by interaction than in the case of CO.

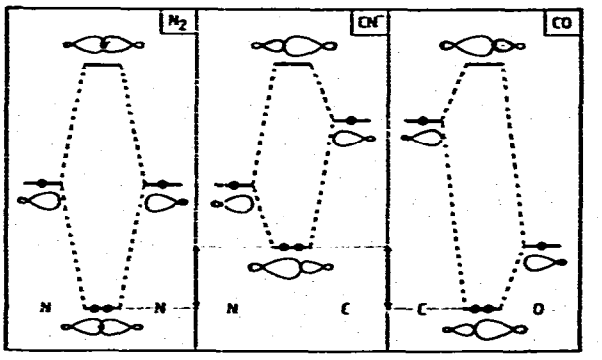

Fig. 6. Schematic representation of the interaction of two atomic sp-hybride functions to form a σ bond in CO, N_2 and CN^-.

resulting in similar relative energy. The situation for CN^- is equivalent to CO but due to the smaller electronegativity of nitrogen, compared to oxygen in CO, the formed σ bond lies at lower relative energy, leading to the apparent destabilization.

Before we proceed to a discussion of absolute ionization energies a brief comment on the relative energies of the outer valence ionizations as compared with the one-particle energies shown in table 1 is appropriate. The relative binding energies of 1π and 5σ orbitals do not fit as well as those discussed for the 3σ orbital. This has to be expected since it is well known that for N_2 a one-particle description of the outer valence ionizations according to Koopmans' theorem is not appropriate [29,30]. The energy separations between the outer valence ionizations observed are not determined by relative one-particle energies but rather by correlation effects [29,30]. Indeed, a comparison of orbital energies for CN^- in table 1 and calculated ionization potentials of table 2 reveal this effect. In the Hartree–Fock calculation with a [12s/8p/2d] basis the 1π–5σ separation is only 0.05 eV. However, upon inclusion of correlation effects the energy separations (table 2) are brought into quantitative agreement with experiment as shown in fig. 5.

The absolute binding energies of the outer valence ionizations are shown at the bottom of fig. 2. The observed values are very close to what has to be expected for a completely ionic NaCN crystal: The first ionization potential (IP) of a CN^- embedded in a NaCN crystal can be calculated from [49]

$$\mathrm{IP} = \mathrm{IP}_{\mathrm{free}}^{\mathrm{CN}^-} + E_{\mathrm{Mad}} + E_{\mathrm{pol}}, \qquad (1)$$

where $\mathrm{IP}_{\mathrm{free}}^{\mathrm{CN}^-}$ is the first ionization potential of the free CN anion. This was experimentally determined by Berkowitz et al. [15] to be 3.82 eV. E_{Mad} is the Madelung energy [50]: 8.07 eV for NaCN. E_{pol} is the polarization energy according to Mott and Littleton [51]. It has been calculated for various anions in connection with ionization of alkali halides and varies between −1 and −2 eV for the anions fluorine to iodine. We have assumed an intermediate value of −1.5 eV. With this we calculate a first ionization potential of 10.4 eV for a completely ionic crystal which is in excellent agreement with the observed value of 10.8 eV. Note that the first ionization potential of free CN^- of 3.82 eV [15] is in excellent agreement with the extended 2ph–TDA result which predicts 4.11 eV and even better when compared with the theoretical value calculated using the OVGF method [29] which is given in parentheses in table 2 (3.81 eV). Note, however, that calculated values are always vertical ionization energies.

The absolute and relative binding energies in the outer valence electron region are independent of excitation energy as revealed by fig. 2. Were the NaCN crystal a "normal" ordered solid then we would observe shifts of the absolute and relative binding energies according to the sampled electron momentum of the "band structure" [1,52]. The absence of the effect is a direct consequence of the disorder within the CN^- sublattice. A detailed photoemission study of absolute and relative binding energies for a NaCN phase with a rotationally ordered CN sublattice would be interesting.

The relative energies for the core ionizations are given in table 3. The N1s spectrum of NaCN is shown for completeness in fig. 7. Note, that we observe shake-up satellite structure on the high binding energy side of the main line at 391.64 eV relative energy. The first intense satellite lies at ≈13 eV excitation energy and corresponds to those observed in the same energy range for CO and N_2. The satellite structure in the core region of CN^- will be discussed in detail elsewhere. The absolute values can be computed referring to the first ionization energy and can be compared to binding energies of other CN containing molecules. For the solid the absolute values are: C1s = 290.3 eV and N1s = 405.8 eV; for the gaseous species: C1s = 283.3 eV and N1s = 398.8 eV. If these values are compared with binding energies of neutral CN compounds in the gas phase: acetonitrile, C1s = 292.4 eV, N1s = 405.6 eV [53]; methylisocyanide, C1s = 292.4 eV, N1s = 406.8 eV [54]; hydrogencyanide, C1s = 293.5 eV, N1s = 406.1 eV [55], the influence of the negative charge is clearly observed. An extensive comparison of core binding energies and shake-up structure of CN^- with (iso-)nitrile, (iso-)nitrile complexes and

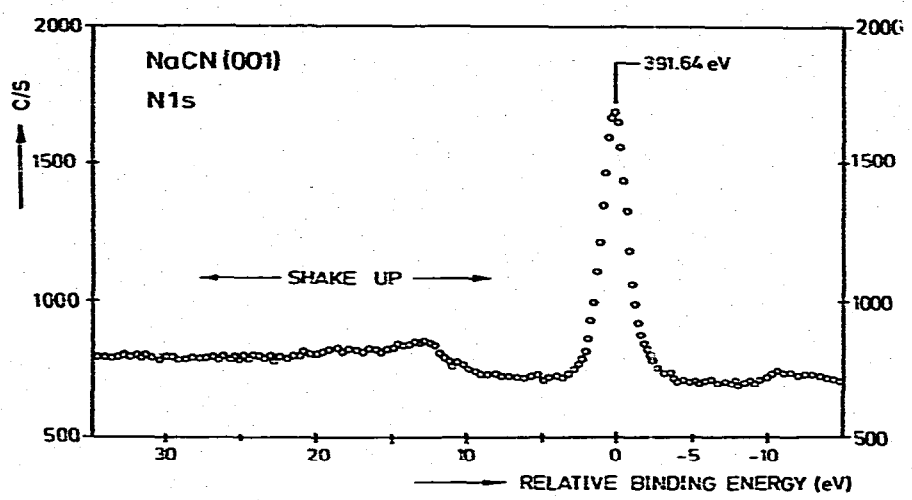

Fig. 7. Core photoelectron spectrum of the N1s level of NaCN. The binding energy is referenced to the 4σ level. Excitation with Si Kα.

(iso-)nitrile adsorbates will be given elsewhere in analogy to our studies on CO- and N_2-complexes and adsorbates [56].

4.2. Branching ratios and shape resonances

So far we have not discussed in detail the intensities of the outer valence electron bands as a function of photon energy. In the following we want to compare the branching ratios of NaCN shown in fig. 3 with those of gaseous and condensed CO and N_2 reported by Plummer et al. [3] and by Fock et al. [2]. [a] Note, however, that the branching ratios for CO and N_2 have been taken with an angle-integrating spectrometer, while our NaCN data were taken in an angle-resolved mode. In order to compare angle-resolved and angle-integrated spectra, a possible influence of the asymmetry parameter β has to be taken into account. Since $\beta(\omega)$ is not known for CN^-, we use the known $\beta(\omega)$ for CO and N_2 and consider its influence on the NaCN spectra. $\beta(\omega)$ varies differently as a function of photon energy for the three ion states in the outer valence electron region. The extreme values are -1 and 2 [57,58]. For both CO and N_2 the smallest value is found for the 1π ionization at 20 eV photon energy with $\beta = -0.5$, the largest value for the 5σ ionization with $\beta = 1.3$ at 40 eV photon energy [58]. If we write the asymmetry-parameter-dependent cross section as

$$d\sigma(\omega, \theta)/d\Omega = (\sigma_{tot}/4\pi) f(\omega, \theta), \quad (2)$$

$$f(\omega, \theta) = \tfrac{1}{2}\beta(\omega)\left[1 + (3\cos^2\theta - 1)\right], \quad (3)$$

where θ is the angle between the polarization vector of the light and the detection direction, then $f(\omega, \theta)$ assumes values between 0.9 and 1.2 for our geometric conditions ($\theta = 45°$). This changes the branching ratios slightly but by no means dramatically. Particularly it does not change the habitus of the frequency dependence of the branching ratios. We conclude that the *structure* we observe in the branching ratios is not primarily caused by the asymmetry parameter.

To assign the various features we compare our results to CO and N_2 in fig. 8 [2,3]. The figure shows for each of the three outer valence ionizations the branching ratios of gaseous and solid CO and N_2 and of CN^- in a photon energy range between 20 eV and 40 eV. For the 5σ ionization at

[a] The pronounced differences between the branching ratios of gaseous and solid CO and N_2 near threshold, which have been discussed in detail by Fock [2], shall not be considered in this paper.

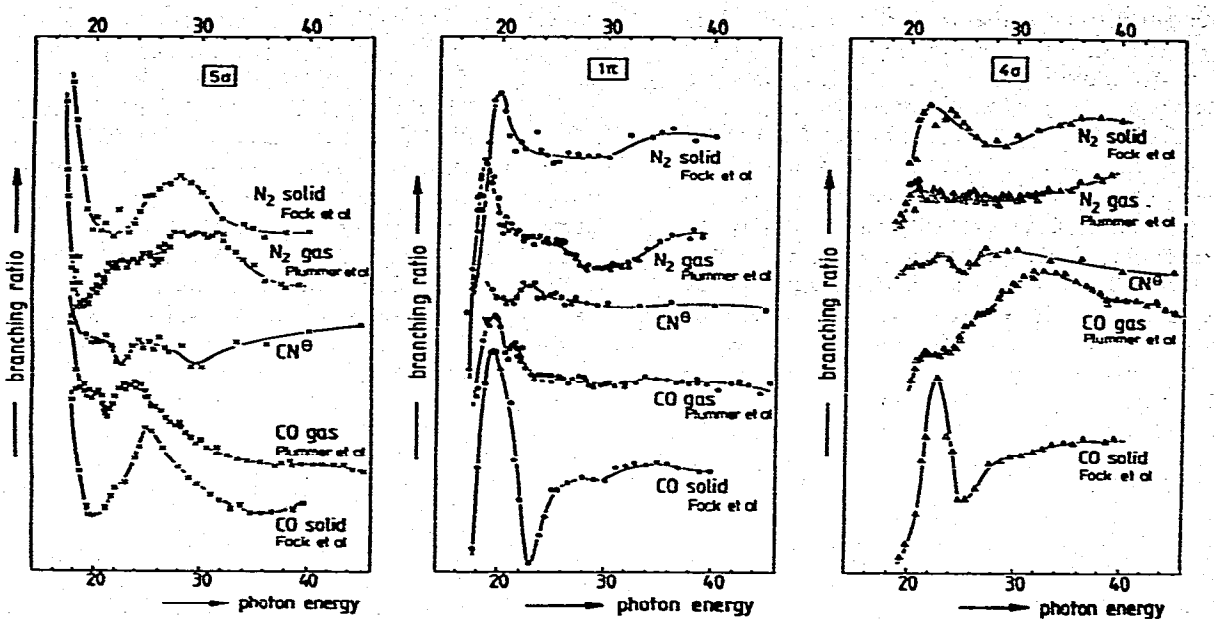

Fig. 8. Comparison of experimental branching ratios of gaseous [3] and solid [2] CO and N_2 with CN^- between 20 and 45 eV photon energy. (a) 5σ ionization. (b) 1π ionization. (c) 4σ ionization. The abscissa is identical for all systems.

low photon energy we find a dip in the branching ratio (22.5 eV) followed by a peak (25.4 eV). A similar structure was found by Plummer et al. [3] for gaseous CO. These authors showed that the features are not primarily the result of autoionization. They argued, that the rise in the branching ratio below the minimum probably is a consequence of autoionization processes involving the $C\,^2\Sigma$ state of CO. This state is seen in photoemission as the shake up at lowest binding energy in fig. 4. Plummer et al. [3] showed, using Davenport's [59] theoretical results that the peak is caused by a σ shape resonance in the continuum. We adopt this interpretation and assign the peak at 25.4 eV photon energy to a shape resonance of σ symmetry. The σ character of the resonance is supported by its absence in the 1π branching ratio, which is basically independent of photon energy except for a small, narrow peak with a maximum near the energy of the dip in the 5σ branching ratio. The same peak in the 1π branching ratio is found in CO and N_2 and it is not clear what causes the variations in cross section. It is possible that interference between comparable amplitudes for autoionization and photoionization is the reason. It is probably not connected directly with the shape resonance, because its width is too small. The branching ratio for the 4σ state also shows a broad resonance feature at 30 eV photon energy. The width of this structure is larger compared to the 5σ branching ratios in accord with findings for CO and N_2. The observation of resonance structures for both σ ionizations is in agreement with the symmetry $C_{\infty v}$ of the CN^- moiety. The intensities of the resonance structures seem to be reduced as compared to gaseous CO and N_2. This effect has also been observed for the 4σ resonance of CO upon condensation [2] of the gas.

In fig. 3 we compare the branching ratios for the NaCN single crystal with those taken from the work of Considine et al. [19]. Their branching ratios were determined for a polycrystalline sample using unpolarized resonance radiation and an angle-integrating spectrometer. The HeI branching ratios agree very well with our findings while for the HeII branching ratios our values agree for the

1π state but differ for the 4σ and 5σ states: while for a polycrystalline sample the branching ratios at 40 eV of 4σ and 5σ are almost identical, they are considerably different for a single-crystalline sample. We do not know what causes the effect but we could speculate that it is due to some orientational order within the CN^- sublattice in the NaCN single crystal. In order to shed light on this problem one could measure the branching ratios when going through the cubic to orthorhombic phase transition at 288 K, because the CN^- sublattice orders in the low-temperature phase. However, it is not easy to retain the single crystallinity of the sample across the phase transition.

Finally, we compare the photon energies of various shape resonances in CO, N_2 and CN^- in table 4. For comparison the values for adsorbed CO and N_2 are included. We find that the photon energies of the CN^- shape resonances are more similar to those of free CO and N_2, than of coordinated CO and N_2.

What causes the shape resonance to shift? A shift of a line is caused by a combination of initial and final state effects. Usually it is not at all easy to differentiate between the two contributions. Only in certain, particularly simple cases, e.g., core ionization in free CO compared to carbonyls [60], has it been possible to actually prove that final state effects dominate. Davenport has already pointed out that a potential change simulated in an $X\alpha$ SW calculation by altering the parameter α leads to changes in the position of the shape resonance [59]. A change in the potential also occurs upon adsorption of a molecule [61]. Very recently, Schichl et al. [62] presented a rather detailed study of the effect of adsorption on the shape resonance using CO–metal cluster models. Greuter et al. [4], earlier, used qualitative arguments and arrived at similar – not as detailed – conclusions. Both groups of authors conclude that chemisorption changes the wavefunctions of the molecule but leave open the answer, whether final or initial states dominate. The present data on CN^- add more evidence to this question. As stated in the introduction, the electron distribution in CN^- is different from CO and N_2. Therefore we can take CN^- as a model to study how wavefunction changes influence the position of the shape resonance. Table 4 shows that a wavefunction change in the case of CN^- does influence the position of the shape resonance but the change is not as large as upon adsorption (see e.g., the 5σ resonance). Therefore it seems as if the apparent shift of the 5σ shape resonance upon adsorption is caused by final rather than initial state effects.

Table 4
Photon energies of shape resonances for the σ levels of various systems in eV. The CO nomenclature is used throughout

System	5σ	4σ	Ref.
CO gas	23.7	32.3	[3]
CO solid	25.3	36.2	[63]
N_2 gas	30.1	–	[3]
N_2 solid	28.0	–	[2]
CN^-	25.3	28.8	
CO/Ni(100)	31.0	36.0	[64]
CO/Co(0001)	31.0	33.2	[4]
CO/Co(0001) high coverage	32.0	36.0	[4]
N_2/Ni(110)	28.5	31.5	[65]

5. Summary and conclusion

We have presented angle-resolved photoelectron spectra of a NaCN (001) single-crystal surface. Synchrotron UV radiation and conventional X-ray tube radiation induced electron distribution curves show that the valence ionization spectra between 10 and 40 eV binding energy are exclusively determined by emission from the CN^- sublattice. The first Na emission (Na2p) appears 23 eV below the 4σ emission. The latter result, together with the measured absolute binding energies support the view that the outer sodium electron has been completely transferred towards the CN moieties which form the CN^- sublattice. Photon-energy-dependent spectra show no variation of absolute and relative binding energies of the CN^- ionizations. This is in agreement with results from neutron diffraction studies [16] showing that the CN^- anions rotate on their lattice positions and thus form a "Coulomb stabilized" CN^- gas.

The satellite structure, observed in the inner valence electron region can be interpreted on the basis of a comparison to condensed CO and N_2

and to many-body corrected calculations on the CN^- anion reported in this paper.

The branching ratios of the outer valence levels show resonance structures in both σ levels, but not in the π level in agreement with the $C_{\infty v}$ symmetry of the CN^- moiety. The position of the shape resonances in CN^- are different from CO and N_2. There is a considerable difference between CN^- and adsorbed CO. It is argued that this is an indication that the apparent shift of the σ resonances is, indeed, basically not an initial but a final state effect.

Acknowledgement

We are grateful to Professor Dr. S. Haussühl for providing the NaCN single crystals. Two of us (HP and HJF) are indebted to Professor Dr. G. Hohlneicher for his continuous support and the possibility to use his LHS10 X-ray photoelectron spectrometer. We would like to thank Professor E.W. Plummer for useful comments on the manuscript.

References

[1] E.W. Plummer and W. Eberhardt, Advan. Chem. Phys. 49 (1982) 533.
[2] J.-H. Fock, H.-J. Lau and E.E. Koch, Chem. Phys. 83 (1984) 377;
H.-J. Lau, J.-H. Fock and E.E. Koch, Chem. Phys. Letters 89 (1982) 281;
J.-H. Fock, Thesis, Hamburg, FRG, (1983), unpublished.
[3] E.W. Plummer, T. Gustafsson, W. Gudat and D.E. Eastman, Phys. Rev. A15 (1977) 2339.
[4] F. Greuter, D. Heskett, E.W. Plummer and H.-J. Freund, Phys. Rev. B27 (1983) 7117.
[5] J. Schirmer, L.S. Cederbaum, W. Domcke and W. von Niessen, Chem. Phys. 26 (1977) 149.
[6] S. Krummacher, V. Schmidt and F. Wuilleumier, J. Phys. B13 (1980) 3993;
S. Krummacher, V. Schmidt, F. Wuilleumier, J.M. Bizau and D. Ederer, J. Phys. B16 (1983) 1733.
[7] W. Eberhardt and H.-J. Freund, J. Chem. Phys. 78 (1983) 700.
[8] R. Bonaccorsi, C. Petrongolo, E. Scrocco and J. Tomasi, J. Chem. Phys. 48 (1968) 1500.
[9] E. Clementi and D. Klint, J. Chem. Phys. 50 (1969) 4899.
[10] J.B. Moffat and H.E. Popkie, J. Mol. Struct. 6 (1970) 155.
[11] K.M. Griffing and J. Simons, J. Chem. Phys. 64 (1976) 3610.
[12] P.R. Taylor, G.B. Bacskay, N.S. Hush and A.C. Hurley, J. Chem. Phys. 70 (1979) 448.
[13] G. Natta and L. Passerini, Gazz. Chim. Ital. 61 (1931) 191.
[14] H.J. Verweel and J.M. Bijvoet, Z. Krist. 100 (1938) 8201.
[15] J. Berkowitz, W.A. Chupka and T.A. Walter, J. Chem. Phys. 50 (1969) 1497.
[16] J.M. Rowe, D.G. Hinks, D.L. Price, S. Susman and J.J. Rush, J. Chem. Phys. 58 (1973) 2039.
[17] J.M. Bijvoet and J.A. Lely, Rec. Trav. Chim. 59 (1940) 908.
[18] See, e.g., S. Haussühl, Solid State Commun. 13 (1973) 147; K. Strässner, W. Henkel, H.D. Hochheimer and M. Cardona, Solid State Commun. 47 (1983) 567;
C.H. Wang and S.K. Satija, J. Chem. Phys. 67 (1977) 851.
[19] M. Considine, J.A. Connor and I.H. Hillier, Inorg. Chem. 16 (1977) 1392.
[20] R. Engelhardt, Diploma Thesis, Hamburg, FRG (1982), unpublished;
C.A. Feldmann, R. Engelhardt, T. Premien, E.E. Koch and V. Saile, Nucl. Instr. Methods 208 (1983) 785.
[21] H.D. Polaschegg, Appl. Phys. 4 (1974) 63.
[22] R.A. Pollak, S.P. Kowalczyk, L. Ley and D.A. Shirley, Phys. Rev. Letters 29 (1972) 274.
[23] B. Marquardt, unpublished results.
[24] S.F. Boys, Proc. Roy. Soc. A200 (1950) 542.
[25] S. Huzinaga, Progr. Theoret. Phys. S40 (1967) 52.
[26] W.J. Hehre, F. Stewart and J.A. Pople, J. Chem. Phys. 51 (1969) 2657.
[27] J.S. Binkley, J.A. Pople and W.J. Hehre, J. Am. Chem. Soc. 102 (1980) 939.
[28] L.S. Cederbaum, Theoret. Chim. Acta 31 (1973) 239; J. Phys. B8 (1975) 290.
[29] L.S. Cederbaum and W. Domcke, Advan. Chem. Phys. 36 (1977) 205.
[30] W. von Niessen, G.H.F. Diercksen and L.S. Cederbaum, J. Chem. Phys. 67 (1977) 4124.
[31] J. Schirmer, L.S. Cederbaum and O. Walter, Phys. Rev. A28 (1983) 1237.
[32] J. Schirmer and L.S. Cederbaum, J. Phys. B11 (1978) 1889.
[33] W. von Niessen, J. Schirmer and L.S. Cederbaum, Comput. Phys. Rept. 1 (1984) 57.
[34] C. Salez and A. Veillard, Theoret. Chim. Acta 11 (1968) 441.
[35] G.H.F. Diercksen and W.P. Kraemer, MUNICH: Molecular program system reference manual, Special Technical Report (Max-Planck-Institut für Physik und Astrophysik, Munich), to be published;
G.H.F. Diercksen, Theoret. Chim. Acta 33 (1974) 1.
[36] N.-G. Vannerberg, Chem. Scripta 9 (1976) 122.
[37] U. Gelius, in: Electron spectroscopy, ed. D.A. Shirley (North-Holland, Amsterdam, 1971).
[38] K. Siegbahn, C. Nordling, G. Johansson, J. Hedman, P.F. Hedin, K. Hamrin, U. Gelius, T. Bergman, L.O. Werme, R. Manne and Y. Baer, ESCA applied to free molecules (North-Holland, Amsterdam, 1971).
[39] R. Prins and P. Biloen, Chem. Phys. Letters 30 (1975) 340.

[40] W.H. Morrison and D.N. Hendrickson, Inorg. Chem. 11 (1972) 2600.
[41] J. Schirmer and O. Walter, Chem. Phys. 78 (1983) 201.
[42] P.W. Langhoff, S.R. Langhoff, T.N. Resigno, J. Schirmer, L.S. Cederbaum, W. Domcke and W. von Niessen, Chem. Phys. 58 (1981) 71.
[43] G. Wendin, Breakdown of one-electron pictures in photoelectron spectra, in: Structure and bonding, Vol. 45 (Springer, Berlin, 1981).
[44] E.N. Lassettre, Can. J. Chem. 47 (1969) 1733.
[45] W. von Niessen and R. Cambi, J. Electron Spectry., to be published.
[46] P.S. Bagus and E.K. Viinikka, Phys. Rev. A15 (1977) 1486.
[47] T. Åberg, Ann. Acad. Sci. Fennicae A6 308 (1969) 1.
[48] L. Pauling, The nature of the chemical bond and the structure of molecules and crystals (Cornell Univ. Press, Ithaca, 1960).
[49] J. Berkowitz, in: The alkali halide vapors, eds. P. Davidovits and D.L. McFadden (Academic Press, New York, 1979).
[50] M. Born and J.E. Mayer, Z. Physik 75 (1932) 1.
[51] N.F. Mott and M.J. Littleton, Trans. Faraday Soc. 34 (1938) 485.
[52] F.J. Himpsel, Appl. Opt. 19 (1980) 3964.
[53] W.L. Jolly and T.F. Schaaf, unpublished results; A.A. Bakke, H.-W. Chen and W.L. Jolly, J. Electron Spectry. 20 (1980) 333.
[54] P. Brant, J. Electron Spectry. 33 (1984) 153.
[55] T.D. Thomas and R.W. Shaw Jr., J. Electron Spectry. 5 (1974) 108.
[56] H.-J. Freund, Habilitationsschrift, Cologne, Fed. Rep. Germany (1983), unpublished.
[57] J.C. Tully, R.S. Berry and B.J. Dalton, Phys. Rev. 176 (1968) 95.
[58] W. Thiel, Chem. Phys. 77 (1983) 103, and references therein.
[59] J.W. Davenport, Phys. Rev. Letters 36 (1976) 945; Thesis, University of Pennsylvania, USA, (1976), unpublished.
[60] H.-J. Freund, E.W. Plummer, W.R. Salaneck and R.W. Bigelow, J. Chem. Phys. 75 (1981).
[61] J.W. Davenport, J. Vac. Sci. Technol. 15 (1978) 433.
[62] A. Schichl, D. Menzel and N. Rösch, Chem. Phys. Letters 105 (1984) 285.
[63] H.-J. Lau, Diploma Thesis, University of Hamburg, FRG, (1982), unpublished; Internal Report HASYLAB 82-01 (March 1982).
[64] C.L. Allyn, T. Gustafsson and E.W. Plummer, Chem. Phys. Letters 47 (1977) 127.
[65] K. Horn, J. DiNardo, W. Eberhardt, H.-J. Freund and E.W. Plummer, Surface Sci. 118 (1982) 465.